

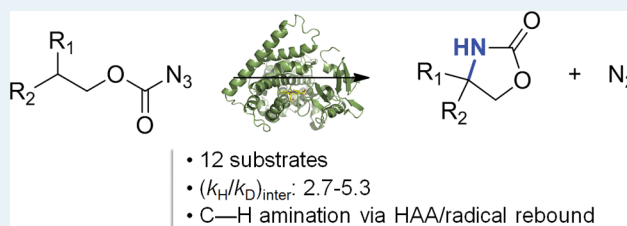
# Enzymatic C(sp<sup>3</sup>)-H Amination: P450-Catalyzed Conversion of Carbonazidates into Oxazolidinones

Ritesh Singh, Joshua N. Kolev, Philip A. Sutera, and Rudi Fasan\*

Department of Chemistry, University of Rochester, Rochester, New York 14627, United States

## Supporting Information

**ABSTRACT:** Cytochrome P450 enzymes can effectively promote the activation and cyclization of carbonazidate substrates to yield oxazolidinones via an intramolecular nitrene C–H insertion reaction. Investigation of the substrate scope shows that while benzylic/allylic C–H bonds are most readily aminated by these biocatalysts, stronger, secondary C–H bonds are also accessible to functionalization. Leveraging this “non-native” reactivity and assisted by fingerprint-based predictions, improved active-site variants of the bacterial P450 CYP102A1 could be identified to mediate the aminofunctionalization of two terpene natural products with high regio- and stereoselectivity. Mechanistic studies and KIE experiments show that the C–H activation step in these reactions is rate-limiting and proceeds in a stepwise manner, namely, via hydrogen atom abstraction followed by radical recombination. This study expands the reactivity scope of P450-based catalysts in the context of nitrene transfer transformations and provides first-time insights into the mechanism of P450-catalyzed C–H amination reactions.



**KEYWORDS:** C–H amination, cytochrome P450, biocatalysis, carbonazidate, oxazolidinones

## 1. INTRODUCTION

Expanding the scope of protein-based catalysts beyond the reaction space encompassed by natural enzymes constitutes an important, and increasingly sought-after goal in biocatalysis.<sup>1–11</sup> A synthetically most valuable transformation is the direct functionalization of aliphatic C–H bonds, which occur ubiquitously in man-made and natural compounds. Of particular interest are methods for the direct conversion of aliphatic C–H bonds into C–N bonds, owing to the abundance of nitrogen functionalities in biologically active molecules.<sup>12,13</sup> Accordingly, significant efforts have been devoted over the past several years to the development of synthetic transition metal catalysts to promote C(sp<sup>3</sup>)-H amination transformations, especially via nitrene C–H insertion.<sup>14–18</sup> In stark contrast, natural enzymes capable of supporting C(sp<sup>3</sup>)-H amination chemistry via direct C–H bond functionalization are extremely rare (e.g., SAM-dependent lysine 2,3-aminomutase)<sup>19</sup> and none is known to catalyze nitrene C–H insertion reactions. This “gap” prompted us and others to develop engineered and artificial biocatalytic systems for promoting this transformation.<sup>7,20–22</sup> In independent studies, our laboratory and the Arnold group demonstrated that engineered cytochrome P450 enzymes containing either a cysteine<sup>7</sup> or a serine-ligated heme<sup>20</sup> can catalyze the intramolecular C–H amination of arylsulfonyl azides with high catalytic efficiency and selectivity. More recently, activation of arylsulfonyl azide substrates for intramolecular C–H amination using alternative hemoprotein-based catalysts<sup>21</sup> as well as for intermolecular sulfimidation<sup>23</sup> was reported.

Based on the promising nitrene transfer reactivity exhibited by engineered variants of CYP102A1 (P450<sub>BM3</sub>)<sup>24</sup> with arylsulfonyl azides,<sup>7</sup> we envisioned the possibility to exploit P450 catalysts for engaging alternative nitrene donors in intramolecular C–H amination processes. In this regard, the construction of oxalidinone rings via cyclative nitrene C–H insertion<sup>25–27</sup> is of particular relevance as these compounds can provide rapid access, upon hydrolysis, to valuable (chiral) 1,2-aminoalcohols, key functional motifs in many bioactive molecules<sup>28</sup> and chiral auxiliaries.<sup>29</sup> To date, this type of transformation has been achieved with rhodium or silver-based catalysts in the presence of carbamate-derived iminodionanes<sup>25,26</sup> or *N*-tosyloxycarbamates<sup>27</sup> as the substrates. Compared to the latter, organic azides represent considerably more attractive nitrene precursors, owing to their high atom economy and the release of environmentally benign N<sub>2</sub> gas as the byproduct of the amination reaction.<sup>18,30</sup> Here, we report that engineered cytochrome P450 enzymes can effectively catalyze the cyclization of carbonazidate substrates to yield oxazolidinones via an intramolecular C–H amination reaction.

## 2. EXPERIMENTAL SECTION

**2.1. Chemical Synthesis.** Synthetic procedures and characterization data for the acyloxycarbamates 1–3, carbonazidates 4, 6–14, 23–24, Z-12, deuterated probe compounds

Received: November 24, 2014

Revised: January 29, 2015

Published: January 29, 2015

**Table 1. C–H Amination Reactivity of Wild-Type CYP102A1 and Variant FL#62 on Different Carbonyl-Based Nitrene Donors<sup>[a]</sup>**

Reaction scheme: 1-4 + P450 (0.2 mol%) + KPi (pH 8.0) → 5 (25°C, 16 hrs)

Entry	Y	Catalyst <sup>[a]</sup>	Turnovers <sup>[b]</sup>
1		Hemin	<0.5
2		CYP102A1	5
3		FL#62	4
4		Hemin	0
5		CYP102A1	4
6		FL#62	7
7		Hemin	0
8		CYP102A1	0
9		FL#62	0
10	—N <sub>3</sub> (4)	Hemin	0
11		CYP102A1	2
12		FL#62	20
13		Rh <sub>2</sub> (OAc) <sub>4</sub>	0
14		Co(TPP)	0

<sup>[a]</sup>Reaction conditions: 20  $\mu$ M P450, 10 mM substrate, 10 mM NADPH. Hemin reactions: 200  $\mu$ M hemin, 10 mM substrate, 10 mM Na<sub>2</sub>S<sub>2</sub>O<sub>4</sub>. Rh<sub>2</sub>(OAc)<sub>4</sub>/Co(TPP) reactions: 5 mol % catalyst, 200 mM 4 in dry toluene. <sup>[b]</sup>As determined by HPLC (SD within 15%).

D-6, D<sub>1</sub>-11, D<sub>2</sub>-11, and the corresponding oxazolidinone and carbamate products are provided as Supporting Information.

**2.2. Protein Expression and Purification.** Wild-type CYP102A1 and its engineered variants were expressed from pCWori-based plasmids containing the P450 gene under the control of an IPTG-inducible promoter (*Bam*HI/*Eco*RI cassette) according to procedures described previously.<sup>31</sup> Typically, cultures of recombinant DH5 $\alpha$  cells were grown at 37 °C (200 rpm) in Terrific Broth (TB) medium supplemented with ampicillin (100 mg/L) until OD<sub>600</sub> reached 1.0 and then induced with 0.25 mM  $\beta$ -D-1-thiogalactopyranoside (IPTG) and 0.3 mM  $\delta$ -aminolevulinic acid (ALA). After induction, cultures were shaken at 150 rpm and 27 °C and harvested after 20 h by centrifugation at 4000 rpm at 4 °C. Cell lysates were prepared by sonication and loaded on Q-Sepharose resin. P450s were eluted using 20 mM Tris, 340 mM NaCl, pH 8.0. After buffer exchange (50 mM potassium phosphate buffer, pH 8.0), the enzymes were stored at –80 °C. P450 concentration was determined from CO-binding difference spectra ( $\epsilon_{450-490} = 91\,000\text{ M}^{-1}\text{ cm}^{-1}$ ). The vector encoding for the thermostable phosphite dehydrogenase (PTDH) variant Opt13 was kindly provided by the Zhao group.<sup>32</sup> PTDH was overexpressed from pET-15b-based vector in BL21(DE3) cells and purified using Ni-affinity chromatography according to the published procedure.<sup>32</sup>

**2.3. P450 Reactions.** The enzymatic reactions were carried out at a 400  $\mu$ L-scale using 5–20  $\mu$ M purified P450 and 10 mM substrate in the presence of a PTDH-based cofactor regeneration system (1  $\mu$ M PTDH, 100  $\mu$ M NADP<sup>+</sup>, 50 mM sodium phosphite). In a typical procedure, a solution containing the cofactor regeneration system in potassium phosphate buffer (50 mM, pH 8.0) was degassed by bubbling argon into the mixture for 5 min in a sealed vial. A buffered solution containing the P450 enzyme was carefully degassed in a similar manner in a separate vial. The two solutions were then mixed together via cannulation. Reactions were initiated by addition of 8  $\mu$ L of azide (from a 0.5 M stock solution in methanol) with a syringe, and the reaction mixture was stirred for 16 h at room temperature under positive argon pressure.

Control reactions with hemin were conducted following an identical procedure with the difference that the P450 was replaced by 80  $\mu$ L of a hemin solution (100  $\mu$ M in DMSO:H<sub>2</sub>O, 1:1) and sodium dithionite (10 mM) was used as the reductant. Prior to chromatographic analysis (see Analytical Methods below), the reaction mixtures were extracted with 400  $\mu$ L CH<sub>2</sub>Cl<sub>2</sub>, followed by evaporation of the organic layer and dissolution of the residue in 100  $\mu$ L MeOH. Calibration curves for quantification of the different oxazolidinones (Figure S4) were generated using authentic standards produced synthetically (see Synthetic Procedures in SI). All measurements were performed in triplicate. For each experiment, negative control samples containing either no enzyme or no reductant were included. For the CO-inactivation experiment, carbon monoxide was bubbled through the reaction mixture containing the P450 enzyme and sodium dithionite prior to addition of the azide substrate. For the natural product substrates (menthol- and borneol-derived carbonazidates), the reaction was quenched by adding excess dithionite, followed by stirring for 24 h before the addition of internal standard and extraction with CH<sub>2</sub>Cl<sub>2</sub>. The organic layer was then analyzed by GC-MS.

**2.4. Analytical Methods.** GC/MS analyses were performed on a Shimadzu GCMS-QP2010 equipped with a RTX-XLB column (30 m  $\times$  0.25 mm  $\times$  0.28  $\mu$ m) and a quadrupole mass analyzer. Separation method: 1  $\mu$ L injection, inj. temp.: 250 °C, detector temp.: 220 °C. Gradient: column temperature set at 50 °C for 1 min, then to 280 °C at 30 °C/min, then to 280 °C for 4 min. Total run time was 13.67 min. Enantiomeric excess was determined by chiral gas chromatography (GC) using a Shimadzu GC-2010 gas chromatograph equipped with a FID detector and a Agilent CYCLOSIL-B column (30 m  $\times$  0.25 mm  $\times$  0.25  $\mu$ m film). Separation method for 4-methyl-4-(p-tolyl)oxazolidin-2-one (15): 1  $\mu$ L injection, injector temp.: 200 °C, detector temp.: 300 °C. Gradient: column temperature set at 150 °C for 0 min, then to 200 °C at 4.5 °C/min, then to 230 °C at 1.5 °C/min, then to 245 °C at 15 °C/min for 8 min. Separation method for 4-phenyl-oxazolidin-2-one (20): 1  $\mu$ L injection, injector temp.: 200 °C,

detector temp: 300 °C. Gradient: column temperature set at 150 °C for 0 min, then to 200 °C at 4.5 °C/min, then to 220 °C at 1 °C/min, then to 245 °C at 15 °C/min for 8 min. HPLC analyses were performed using a Shimadzu LC-2010A-HT equipped with a VisionHT-C<sub>18</sub> reverse-phase column and a multidiode UV–VIS detector. Injection volume: 10  $\mu$ L. Flow rate: 1 mL/min. Gradient: 10% acetonitrile in water (0.1% TFA) for 3 min, then increased to 90% over 24 min.

**2.5. Kinetic Isotope Effect (KIE) Experiments.** P450 reactions were carried out at a 400  $\mu$ L-scale using 20  $\mu$ M P450, 10 mM NADPH and stopped after 1 h. For KIE determination with **6** and **D-6**, parallel reactions with either of the carbonazidate substrates were carried out at varying substrate concentration (100  $\mu$ M to 2 mM). The reactions were analyzed by HPLC and KIE values were calculated from the resulting plots of initial rate against substrate concentration. For the intra- and intermolecular KIE analyses with **D**<sub>1</sub>-**11** and with equimolar mixtures of **11** and **D**<sub>2</sub>-**11**, respectively, the reactions were carried out as described above using 10 mM total substrate concentration, followed by GC-MS analysis. KIE values were determined based on the ratios between the relative abundances of the characteristic fragments with *m/z* of 105 (nondeuterated) and *m/z* of 106 (deuterated) (Figure S5). Authentic standards of product **20** and **D-20** injected individually and in equimolar mixture were used as references (Figure S5).

### 3. RESULTS AND DISCUSSION

In preliminary experiments, a series of oxycarbonyl-based nitrene donors were prepared using 2-phenylpropanol derivatives as model substrates (Table 1). These compounds comprised acetoxy- (**1**) and aryloxy-carbamate (**2**, **3**) derivatives, which have been previously investigated in the context of rhodium-catalyzed nitrene transfer reactions.<sup>27</sup> Given the ability of P450s to activate sulfonyl azides,<sup>7</sup> the carbonazidate derivative **4** was also synthesized. In addition to being readily accessible from a synthetic standpoint, carbonazidates are most desirable precursors for oxazolidinone formation via nitrene C–H insertion because of their high atom economy, with N<sub>2</sub> being produced as byproduct as opposed to AcOH or ArOH with **2** or **3**. Despite these favorable features and the successful application of carbonazidates in the context of sulfimidation,<sup>33,34</sup> olefin aziridination,<sup>35,36</sup> and aminohalogenation,<sup>33,37</sup> catalytic intramolecular C–H amination reactions involving these compounds have not been reported to our knowledge. CYP102A1 variant FL#62 was chosen for the initial scouting experiments. Compared to wild-type CYP102A1, FL#62 contains five active site mutations (V78A, F81S, A82 V, F87A, A184 V), which contribute to expand its active site and make it accessible to large and bulky substrates.<sup>31,38,39</sup> In addition, FL#62 exhibited the highest C–H amination activity in the presence of arylsulfonyl azides in our previous studies.<sup>7</sup>

P450 reactions with substrates **1**–**4** were performed in the presence of NADPH, to reduce the enzyme to its ferrous state, and anaerobically, both of which conditions were previously found to be critical for supporting P450-dependent nitrene transfer reactivity.<sup>7</sup> Gratifyingly, both wild-type CYP102A1 and FL#62 were found to yield appreciable amounts of the desired oxazolidinone **5** in the presence of the acetoxy- and aryloxy-carbamates **1**–**3** (turnover number (TON): 4–7, Table 1). Importantly, significantly better conversion to the oxazolidinone product could be achieved from the carbonazidate substrate **4** (Table 1) with FL#62 as the catalyst. In contrast,

little or no cyclic product was formed in the presence of wild-type CYP102A1 or free hemin. Notably, no reaction was observed in the presence of **4** under standard amination conditions in the presence of Rh<sub>2</sub>(OAc)<sub>4</sub>, as noted previously,<sup>27</sup> or Co-(TPP) (TPP = tetraphenylporphyrin), two prominent organometallic catalysts investigated in the context of C–H amination reactions.<sup>16,40</sup>

Toward optimization of the reaction conditions, the importance of the source of reducing equivalents in the P450-catalyzed conversion of carbonazidate **4** was investigated. These experiments showed that cyclization of **4** could be achieved by replacing NADPH with the inexpensive dithionite (Na<sub>2</sub>S<sub>2</sub>O<sub>4</sub>), albeit only with lower efficiency (5 vs 20 TON). This difference could be attributed to the kinetically competitive reduction of the carbonazidate substrate to the corresponding carbamate by action of the inorganic reductant as compared to the enzymatic C–H amination reaction (0.2 turnovers/min). More promisingly, comparable number of turnovers as observed in the presence of an excess of NADPH (10 mM) could be obtained using catalytic amounts of NADPH (100  $\mu$ M) in combination with a phosphite dehydrogenase<sup>32</sup> based cofactor regeneration system. Thus, under optimized conditions, over 70 catalytic turnovers were achieved for the FL#62-catalyzed transformation of **4** into **5** (Entry 1, Table 2). These improvements notwithstanding, the yield of the C–H amination product remained moderate (~4%), with the remainder of the carbonazidate substrate being converted to a carbamate and alcohol products as discussed in more details later.

**3.1. Investigation of Substrate Scope.** To gain insights into the influence of electronic and steric effects on the P450-catalyzed C–H amination reaction, a range of carbonazidates (**6**–**10**) were then prepared and tested for cyclization in the presence of FL#62. As shown in Table 2, various substitutions at the level of the aromatic ring of the substrate were tolerated by the enzyme, resulting in turnover numbers ranging from 10 to 100 (Entries 1–6, Table 2). Interestingly, an increase in TON was observed upon substitution of the *para* position with a methyl group (**6**; 100 vs 74 TON), whereas a reduction in C–H amination activity resulted from substitution of this site with an isosteric but electronwithdrawing trifluoromethyl group (**7**; 43 TON). This trend in reactivity is consistent with the electrophilic character of the reactive species envisioned to mediate these reactions (vide infra). Notably, derivatives with a bulky substituent (*tert*-butyl) at the *para* position (**8**) as well as double substitutions on the aromatic ring (**10**) were also processed by the enzyme.

With compounds **11**–**14**, the influence of the relative strength of the target C–H bond on the efficiency of the reaction was investigated. Interestingly, FL#62-mediated amination of the secondary, benzylic C–H bond in **11** as well as in the more conformationally rigid **13** was found to occur with significantly lower efficiency (10-fold) as compared to the tertiary, benzylic C–H site in **4** (5–6 vs 74 turnovers). These results suggest a clear dependence of the P450-dependent amination activity on the C–H bond strength, a conclusion further supported by the comparatively higher activity of the enzyme on **12** (15 TON), and lack of activity on **14**, in which the C–H bonds in  $\beta$  to the carbonazidate group have estimated bond dissociation energies (BDE) of 86 and 98 kcal/mol, respectively.<sup>41</sup> This bias notwithstanding, the catalytic turnovers achieved by these P450 catalysts with carbonazidates compare very favorably with those reported for rhodium or

**Table 2.** Scope of P450-Catalyzed C–H Amination with Carbonazidate Substrates<sup>[a]</sup>

Entry	Substrate	Product	TON
1	<b>4</b>	<b>5</b>	74 ± 8
2	R <sub>1</sub> = Me; R <sub>2</sub> = <i>p</i> -Tol ( <b>6</b> )	<b>15</b>	100 ± 4
3	R <sub>1</sub> = Me; R <sub>2</sub> = 4-CF <sub>3</sub> -Ph ( <b>7</b> )	<b>16</b>	43 ± 2
4	R <sub>1</sub> = Me; R <sub>2</sub> = 4-tBu-Ph ( <b>8</b> )	<b>17</b>	7 ± 1
5	R <sub>1</sub> = H; R <sub>2</sub> = <i>m</i> -Tol ( <b>9</b> )	<b>18</b>	23 ± 2
6	R <sub>1</sub> = H; R <sub>2</sub> = 3,5-dimethyl-phenyl ( <b>10</b> )	<b>19</b>	10 ± 1
7	R <sub>1</sub> = H; R <sub>2</sub> = Ph ( <b>11</b> )	<b>20</b>	5 ± 1
8	R <sub>1</sub> = H; R <sub>2</sub> = CH <sub>2</sub> -CH=CH-Ph ( <b>12</b> )	<b>21</b>	15 ± 2
9	<b>13</b>	<b>22</b>	6 ± 1
10	<b>14</b>	no oxazolidinone product	0

<sup>[a]</sup>Reactions conditions: 5 μM P450, 10 mM carbonazidate, cofactor regeneration system (100 μM NADP<sup>+</sup>, 1 μM phosphite dehydrogenase, 50 mM Na<sub>2</sub>PO<sub>3</sub>), 16 h. Turnover numbers (TON) were measured by HPLC from triplicate experiments.

silver catalysts in the context of oxazolidinone synthesis from carbamate-iminoiodinane or *N*-tosyloxy-carbamate precursors (5–25 turnovers).<sup>25–27</sup> Furthermore, the absence of aziridine formation in the reaction with **12** supports the chemoselectivity of the P450 catalyst toward nitrene C–H insertion over the potentially competing aziridination reaction.<sup>27,42</sup>

Chiral analysis of the oxazolidinone products generated from **4**, **8**, and **11** in the presence of FL#62 showed only low levels of enantioinduction (2–5% ee). These results were rather surprising as moderate to high degree of stereo- or enantioselectivity (40–91% ee) were observed in the cyclization of arylsulfonyl azides by means of FL#62 and related CYP102A1 variants.<sup>7</sup> Screening of a panel of 15 FL#62-derived active site variants against carbonazidates **4**, **8**, and **11** gave similar results, suggesting that the limited chiral induction observed with these substrates is not dependent upon the active site configuration of the enzyme but it is rather linked to the mechanism of the C–H activation step operating in these processes as discussed further below.

**3.2. Natural Product Substrates.** To further investigate the scope and potential utility of the P450 catalysts in the context of oxazolidinone synthesis, carbonazidate derivatives of

two natural product terpenes, menthol (**23**) and borneol (**24**), were subjected to FL#62 catalysis (Figure 1). Notably, both

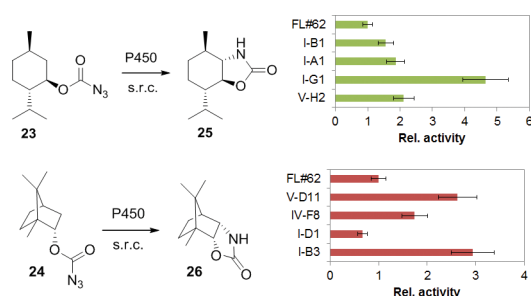


**Figure 1.** P450-catalyzed C–H amination in terpene natural products. The graphs illustrate the relative activity, based on TON, for the FL#62-derived active-site variants selected by fingerprint analysis (SCA). The amino acid mutations in the P450 variants can be found in Table S1. “s.r.c.” = standard reaction conditions, as indicated in Table 2.

compounds could be converted to a single five-membered cyclic product, namely, the *trans*-oxazolidinone **25** and the *cis*-oxazolidinone **26**, respectively, with high regio- and stereo-selectivity. The high degree of site-selectivity obtained in the reactions with these substrates contrasts with the unselective nitrene C–H insertion events observed upon pyrolysis or photolysis of related compounds.<sup>43,44</sup>

Despite the successful cyclization of **23** and **24**, we noted that the catalytic efficiency of FL#62 on these substrates was only modest (TON ~ 4). Recently, we reported a fingerprint-based method for predicting the substrate reactivity of engineered P450s on target molecules that are structurally related to the probe compounds used for their fingerprinting (referred to as “fingerprint single component analysis” or SCA).<sup>38,39</sup> Substrates **23** and **24** share significant scaffold similarity with two of said fingerprint probes, namely, the cyclohexane- and the bornane-based probes (Figure S1). Using SCA, four candidate P450 catalysts with potentially improved activity for the cyclization of these substrates were identified from our previously assembled collection of FL#62-based variants, which were derived from this P450 via simultaneous mutagenesis of 2 to 6 active site positions.<sup>31,39</sup> Gratifyingly, these P450s were found capable of processing **23** and **24** supporting 3- to 5-fold higher catalytic turnovers than FL#62 (Figure 2). Altogether, these studies demonstrate the possibility to apply these P450 catalysts for

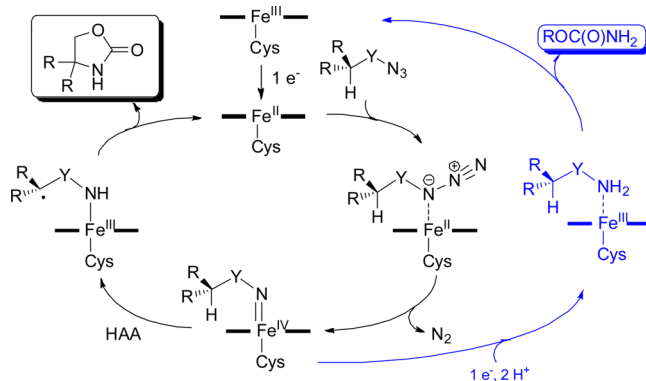


**Figure 2.** Proposed mechanism for P450-catalyzed conversion of carbonazidates to oxazolidinones. The competing pathway leading to the carbamate byproduct is indicated in blue. Y = —OC(O)—.

C–H amination transformations in the context of structurally and stereochemically complex molecules. Furthermore, these results support the functionality of our fingerprint-based methods for P450 substrate reactivity prediction also in the context of P450-mediated C–H aminations.

**3.3. Mechanistic Studies.** Further experiments were conducted to shed light into the mechanism of these reactions. The requirement for a reductant (i.e., dithionite or NADPH) and complete loss of carbonazidate C–H amination activity upon complexation of the reduced P450 with CO provided clear evidence in support of the involvement of the ferrous heme in catalysis. Accordingly and building upon our investigations with arylsulfonyl azides<sup>7</sup> and previous studies with metalloporphyrin systems,<sup>45–48</sup> we envision the catalytic cycle to initiate with the binding of the carbonazidate substrate to the ferrous heme to form an azido-iron(II) complex, which would then undergo nitrogen loss to give a putative imido-iron(IV) intermediate (Figure 2). Reasonably, the subsequent C–H activation event could then proceed through (a) a stepwise hydrogen atom abstraction (HAA)/radical rebound mechanism, analogous to that mediated by oxo-iron(IV)-porphyrin  $\pi$  cation radical (Compound I) in P450-catalyzed C–H oxidations,<sup>49,50</sup> or (b) a concerted nitrene C–H insertion, analogous to that operating in rhodium-catalyzed C–H aminations.<sup>51</sup> To probe this step, the *cis* isomer of carbonazidate **12** ((*Z*)-**12**, Figure 3) was subjected to FL#62-

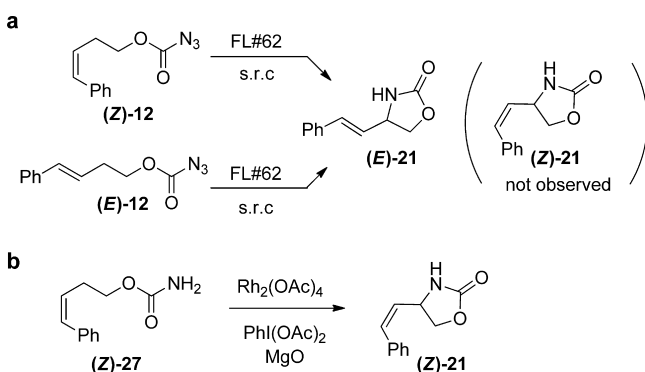


**Figure 3.** Rearrangement studies. (a) FL#62-catalyzed cyclization of (*E*)-**12** (or its isomer (*Z*)-**12**) leads to formation of *trans* oxazolidinone (*E*)-**21**, as determined by HPLC (Figure S3 in SI) and GC-MS analysis. The *Z*  $\rightarrow$  *E* rearrangement in case of (*Z*)-**12** is indicative of the formation radical intermediate via HAA. (b) Rhodium-catalyzed cyclization of carbamate **Z-27** is not accompanied by scrambling of the double bond configuration, in agreement with the concerted nitrene C–H insertion mechanism proposed for these catalysts.<sup>51</sup>

catalyzed amination conditions, with scrambling of the double bond geometry upon cyclization being revealing of a radical mechanism. Interestingly, only formation of the rearranged *trans* oxazolidinone (*E*)-**21** was observed (TON: 16), a product identical to that generated starting from (*E*)-**12** (Figure 3). In contrast, rhodium-catalyzed cyclization of carbamate (*Z*)-**27** activated in situ with  $\text{PhI}(\text{OAc})_2$  yielded the *cis* oxazolidinone product (*Z*)-**21**. Thus, these results unambiguously revealed that a stepwise mechanism, involving HAA followed by radical recombination, is operative in the P450 amination reaction (Figure 2). Furthermore, the complete *Z*  $\rightarrow$  *E* rearrangement of the olefinic bond in (*Z*)-**12** is suggestive of the formation of a relatively long-lived carbon-centered radical, which could

account for the observed lack of stereo/enantioselectivity upon amination of the benzylic C–H sites in **4**, **8**, and **11** by FL#62 and its variants. On the other hand, the high stereoselectivity observed in the case of the menthol and borneol derivatives (Figure 1) could stem from the faster rebound step expected to occur for the less stabilized secondary alkyl radical intermediate formed during the intramolecular C–H amination of these substrates.

**3.4. Kinetic Isotope Effect (KIE) Experiments.** According to the mechanistic model of Figure 2, cleavage of the C–H bond was expected to be rate-limiting during oxazolidinone formation. To examine this aspect, the effect of H/D substitution on the C–H amination rate of substrate **6** was determined (Figure 4a). The positive primary kinetic isotope

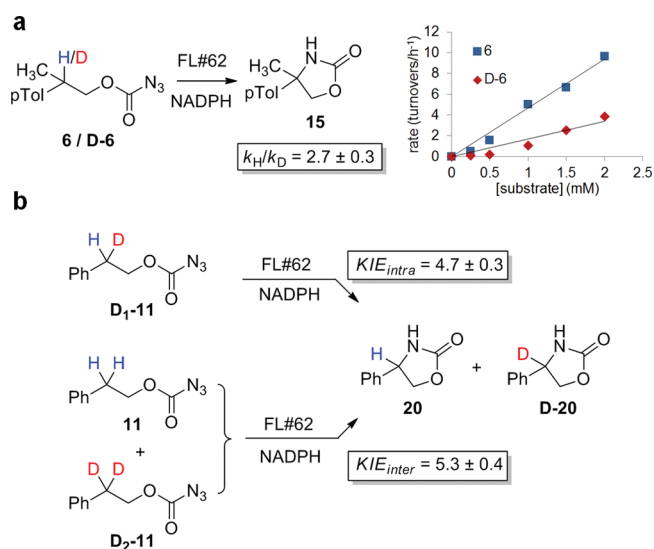


**Figure 4.** Kinetic isotope effect (KIE) experiments. (a) KIE value for FL#62-catalyzed amination of **6** and its deuterated analogue, **D-6**. The graph reports a plot of initial rate versus substrate concentration for the two reactions. (b) Comparison of  $\text{KIE}_{\text{intra}}$  and  $\text{KIE}_{\text{inter}}$  values as determined from intramolecular (**D<sub>1</sub>-11**) and intermolecular (1:1 mixture of **11** and **D<sub>2</sub>-11**) competition experiments, followed by GC-MS analysis (Figure S5).

effect observed in these experiments ( $k_{\text{H}}/k_{\text{D}}$ :  $2.7 \pm 0.3$  at 20 °C) is consistent with the involvement of C–H bond cleavage in the rate-determining step of the reaction. At the same time, this value is considerably smaller than and comparable to, respectively, that observed for C–H amination reactions with Ru-porphyrins ( $k_{\text{H}}/k_{\text{D}}$ : 6–12)<sup>46,52</sup> and rhodium catalysts ( $k_{\text{H}}/k_{\text{D}}$ : 1.8–4.5),<sup>51,53</sup> which were established to operate via a stepwise and concerted C–H activation pathway, respectively. In light of the large KIE difference compared to the Ru-porphyrin system, we wondered whether other steps prior to C–H bond cleavage (e.g., activation of the azide via  $\text{N}_2$  extrusion; Figure 2), may be also kinetically relevant in the P450 reaction, thus resulting in partial “masking” of the actual KIE associated with the C–H activation step. A powerful approach to examine this aspect is through comparison of  $\text{KIE}_{\text{intra}}$  versus  $\text{KIE}_{\text{inter}}$ .<sup>54,55</sup> Accordingly, the mono- (**D<sub>1</sub>-11**) and *gem*-dideuterated (**D<sub>2</sub>-11**) analogues of compound **11** (Figure 3b) were synthesized (see SI for details) and utilized in intra- and intermolecular competition experiments, respectively. Expectedly, a  $\text{KIE}_{\text{intra}} > \text{KIE}_{\text{inter}}$  would reveal that azide activation is also rate-limiting, whereas  $\text{KIE}_{\text{intra}} \approx \text{KIE}_{\text{inter}}$

would indicate that C–H bond cleavage is the only rate-determining step in the reaction. Analysis of the FL#62-catalyzed cyclization of **D**<sub>1</sub>-**11** yielded a  $KIE_{\text{intra}} = 4.7 \pm 0.3$ , whereas the competition experiment with a 1:1 mixture of **11** and **D**<sub>2</sub>-**11** yielded a  $KIE_{\text{inter}}$  value of  $5.3 \pm 0.4$  (Figure 3b), as determined by mass spectrometry (Figure S5). The close similarity between these values (within experimental error) thus supports a scenario in which C–H bond cleavage is likely to be the predominant rate-determining step in these P450-catalyzed C–H amination reactions. At the same time, it is possible that in the presence of weaker C–H bonds (e.g., tertiary vs secondary C–H bond in **6** vs **11**) other steps may become kinetically important, thereby affecting the extent of the KIE associated with the H/D substitution at the level of the aminated C–H bond.

**3.5. Competing Pathways.** Whereas the studies above provided insights into the productive pathway leading to oxazolidinone formation, evidence for the occurrence of competing, unproductive pathways was also gathered. Indeed, in addition to the oxazolidinone product, a considerable amount of the acyclic carbamate and of the corresponding alcohol was observed in the P450 reactions with all the substrates tested. Whereas the carbonazidate is completely consumed in these reactions, the carbamate and alcohol products were found to account for the majority of the consumed substrate (~90%). Nearly complete (>95%) suppression of either byproduct in the presence of CO-saturated buffer proved that they are both generated at the level of the heme center in the enzyme and not from reaction with the flavins in the reductase domain or components of the cofactor regeneration system. As proposed in the context of our previous studies with arylsulfonyl azides, where a similar reduction byproduct (i.e., sulfonamide) was observed,<sup>7</sup> we suspect the acyclic carbamate to originate from overreduction and protonation of the imido-iron intermediate (blue path, Figure 2), a process potentially favored by the native two single-electron/proton transfer mechanism operating in P450s as required for the reductive activation of O<sub>2</sub> to Compound I.<sup>50</sup> Interestingly, a similar “uncoupling” phenomenon was observed during P450-catalyzed nitrene transfer to sulfides recently investigated by Arnold and co-workers.<sup>23</sup> Possible pathways leading to the alcohol byproduct could involve hydrolysis of the heme bound carbonyl-nitrenoid species or radical decarboxylation during catalysis. Although these uncoupling mechanisms currently limit the synthetic utility of these P450-catalyzed transformations, we anticipate that targeting structural elements mediating the native electron/proton transfer pathway in these enzymes could provide a future avenue to further increase their efficiency as C–H amination catalysts.

## 4. CONCLUSIONS

In conclusion, we have reported the successful synthesis of oxazolidinones via the P450-catalyzed cyclization of carbonazidates. In addition to expanding the reaction scope of cytochrome P450 enzymes, this report describes the first example in which these atom-economical and readily accessible nitrene donors are successfully employed in catalytic intramolecular C–H amination reactions. Our structure–reactivity analyses indicate that whereas benzylic/allylic C–H bonds with a BDE < 90 kcal/mol are most readily aminated by these biocatalysts, activation of stronger C–H bonds (i.e., non-benzylic/nonallylic 2 °C–H) is also feasible. Our mechanistic and KIE analyses indicate that the C–H activation step is rate-

limiting and proceeds in a stepwise manner (i.e., via HAA/radical rebound), reminiscent of that involved in P450 hydroxylations. Overall, these studies provide first-time insights into the mechanism of P450-mediated C–H amination as well as a basis for further optimization of these catalysts. The experiments with the terpene substrates demonstrate the feasibility of applying these P450-based amination catalysts for the transformation of complex natural products, with active site mutagenesis providing a way to improve the catalytic activity toward a particular target substrate. Because carbonazidates can be readily synthesized from alcohols, the reactivity reported here could open exciting opportunities for the application of these enzymes in synthesis, which may include, for example, coupling selective P450 hydroxylation<sup>31,39,56</sup> with P450-catalyzed carbonazidate cyclization to install 1,2-aminoalcohol functionalities at remote C(sp<sup>3</sup>)–H positions in organic molecules.

## ■ ASSOCIATED CONTENT

### Supporting Information

The following file is available free of charge on the ACS Publications website at DOI: 10.1021/cs5018612.

Synthetic procedures, compound characterization data and NMR spectra, additional figures and tables (PDF)

## ■ AUTHOR INFORMATION

### Corresponding Author

\*E-mail: fasan@chem.rochester.edu.

### Funding

This work was supported by the U.S. National Institute of Health (R01 grant GM098628). MS instrumentation was supported by the U.S. NSF grant CHE-0946653.

### Notes

The authors declare no competing financial interest.

## ■ REFERENCES

- (1) Wilson, M. E.; Whitesides, G. M. *J. Am. Chem. Soc.* **1978**, *100*, 306–307.
- (2) Collot, J.; Gradinaru, J.; Humbert, N.; Skander, M.; Zocchi, A.; Ward, T. R. *J. Am. Chem. Soc.* **2003**, *125*, 9030–9031.
- (3) Reetz, M. T.; Peyralans, J. J. P.; Maichele, A.; Fu, Y.; Maywald, M. *Chem. Commun.* **2006**, 4318–4320.
- (4) Abe, S.; Niemeyer, J.; Abe, M.; Takezawa, Y.; Ueno, T.; Hikage, T.; Erker, G.; Watanabe, Y. *J. Am. Chem. Soc.* **2008**, *130*, 10512–10514.
- (5) Mayer, C.; Gillingham, D. G.; Ward, T. R.; Hilvert, D. *Chem. Commun.* **2011**, 47, 12068–12070.
- (6) Coelho, P. S.; Brustad, E. M.; Kannan, A.; Arnold, F. H. *Science* **2013**, *339*, 307–310.
- (7) Singh, R.; Bordeaux, M.; Fasan, R. *ACS Catal.* **2014**, *4*, 546–552.
- (8) Yang, H.; Srivastava, P.; Zhang, C.; Lewis, J. C. *ChemBioChem* **2014**, *15*, 223–227.
- (9) Lewis, J. C. *ACS Catal.* **2013**, *3*, 2954–2975.
- (10) Sreenilayam, G.; Fasan, R. *Chem. Commun.* **2015**, *51*, 1532–1534.
- (11) Bordeaux, M.; Tyagi, V.; Fasan, R. *Angew. Chem., Int. Ed.* **2014**, *54*, 1744–1748.
- (12) Dick, A. R.; Sanford, M. S. *Tetrahedron* **2006**, *62*, 2439–2463.
- (13) Davies, H. M. L.; Manning, J. R. *Nature* **2008**, *451*, 417–424.
- (14) Muller, P.; Fruit, C. *Chem. Rev.* **2003**, *103*, 2905–2919.
- (15) Collet, F.; Dodd, R. H.; Dauban, P. *Chem. Commun.* **2009**, 5061–5074.
- (16) Roizen, J. L.; Harvey, M. E.; Du Bois, J. *Acc. Chem. Res.* **2012**, *45*, 911–922.

- (17) Jeffrey, J. L.; Sarpong, R. *Chem. Sci.* **2013**, *4*, 4092–4106.
- (18) Driver, T. G. *Org. Biomol. Chem.* **2010**, *8*, 3831–3846.
- (19) Frey, P. A.; Magnusson, O. T. *Chem. Rev.* **2003**, *103*, 2129–2148.
- (20) McIntosh, J. A.; Coelho, P. S.; Farwell, C. C.; Wang, Z. J.; Lewis, J. C.; Brown, T. R.; Arnold, F. H. *Angew. Chem., Int. Ed.* **2013**, *52*, 9309–9312.
- (21) Bordeaux, M.; Singh, R.; Fasan, R. *Bioorg. Med. Chem.* **2014**, *22*, 5697–5704.
- (22) Hyster, T. K.; Farwell, C. C.; Buller, A. R.; McIntosh, J. A.; Arnold, F. H. *J. Am. Chem. Soc.* **2014**, *136*, 15505–15508.
- (23) Farwell, C. C.; McIntosh, J. A.; Hyster, T. K.; Wang, Z. J.; Arnold, F. H. *J. Am. Chem. Soc.* **2014**, *136*, 8766–8771.
- (24) Narhi, L. O.; Fulco, A. J. *J. Biol. Chem.* **1987**, *262*, 6683–6690.
- (25) Espino, C. G.; Du Bois, J. *Angew. Chem., Int. Ed.* **2001**, *40*, 598–600.
- (26) Cui, Y.; He, C. *Angew. Chem., Int. Ed.* **2004**, *43*, 4210–4212.
- (27) Lebel, H.; Huard, K.; Lectard, S. *J. Am. Chem. Soc.* **2005**, *127*, 14198–14199.
- (28) Kotti, S. R. S.; Timmons, C.; Li, G. G. *Chem. Biol. Drug Des.* **2006**, *67*, 101–114.
- (29) Ager, D. J.; Prakash, I.; Schaad, D. R. *Chem. Rev.* **1996**, *96*, 835–875.
- (30) Intrieri, D.; Zardi, P.; Caselli, A.; Gallo, E. *Chem. Commun.* **2014**, *50*, 11961.
- (31) Zhang, K. D.; Shafer, B. M.; Demars, M. D.; Stern, H. A.; Fasan, R. *J. Am. Chem. Soc.* **2012**, *134*, 18695–18704.
- (32) McLachlan, M. J.; Johannes, T. W.; Zhao, H. *Biotechnol. Bioeng.* **2008**, *99*, 268–274.
- (33) Bach, T.; Schlummer, B.; Harms, K. *Chemistry* **2001**, *7*, 2581–2594.
- (34) Tamura, Y.; Uchida, T.; Katsuki, T. *Tetrahedron Lett.* **2003**, *44*, 3301–3303.
- (35) Bergmeier, S. C.; Stanchina, D. M. *J. Org. Chem.* **1999**, *64*, 2852–2859.
- (36) Bergmeier, S. C.; Stanchina, D. M. *J. Org. Chem.* **1997**, *62*, 4449–4456.
- (37) Kamon, T.; Shigeoka, D.; Tanaka, T.; Yoshimitsu, T. *Org. Biomol. Chem.* **2012**, *10*, 2363–2365.
- (38) Zhang, K.; El Damaty, S.; Fasan, R. *J. Am. Chem. Soc.* **2011**, *133*, 3242–3245.
- (39) Kolev, J. N.; O'Dwyer, K. M.; Jordan, C. T.; Fasan, R. *ACS Chem. Biol.* **2014**, *9*, 164–173.
- (40) Lu, H.; Zhang, X. P. *Chem. Soc. Rev.* **2011**, *40*, 1899–1909.
- (41) Luo, Y. *Handbook of Bond Dissociation Energies in Organic Compounds*; CRC Press LLC: Boca Raton, FL, 2003.
- (42) Padwa, A.; Flick, A. C.; Leverett, C. A.; Stengel, T. *J. Org. Chem.* **2004**, *69*, 6377–6386.
- (43) Banks, M. R.; Blake, A. J.; Cadogan, J. I. G.; Dawson, I. M.; Gosney, I.; Grant, K. J.; Gaur, S.; Hodgson, P. K. G.; Knight, K. S.; Smith, G. W.; Stevenson, D. E. *Tetrahedron* **1992**, *48*, 7979–8006.
- (44) Meth-Cohn, O. *Acc. Chem. Res.* **1987**, *20*, 18–27.
- (45) Mansuy, D.; Battioni, P.; Mahy, J. P. *J. Am. Chem. Soc.* **1982**, *104*, 4487–4489.
- (46) Au, S. M.; Huang, J. S.; Yu, W. Y.; Fung, W. H.; Che, C. M. *J. Am. Chem. Soc.* **1999**, *121*, 9120–9132.
- (47) Fantauzzi, S.; Gallo, E.; Caselli, A.; Ragaini, F.; Casati, N.; Macchi, P.; Cenini, S. *Chem. Commun.* **2009**, 3952–3954.
- (48) Lyaskovskyy, V.; Suarez, A. I. O.; Lu, H. J.; Jiang, H. L.; Zhang, X. P.; de Bruin, B. *J. Am. Chem. Soc.* **2011**, *133*, 12264–12273.
- (49) Groves, J. T.; McClusky, G. A.; White, R. E.; Coon, M. J. *Biochem. Biophys. Res. Commun.* **1978**, *81*, 154–160.
- (50) Denisov, I. G.; Makris, T. M.; Sligar, S. G.; Schlichting, I. *Chem. Rev.* **2005**, *105*, 2253–2277.
- (51) Fiori, K. W.; Espino, C. G.; Brodsky, B. H.; Du Bois, J. *Tetrahedron* **2009**, *65*, 3042–3051.
- (52) Leung, S. K.; Tsui, W. M.; Huang, J. S.; Che, C. M.; Liang, J. L.; Zhu, N. *J. Am. Chem. Soc.* **2005**, *127*, 16629–16640.
- (53) Collet, F.; Lescot, C.; Liang, C.; Dauban, P. *Dalton Trans.* **2010**, 39, 10401–10413.
- (54) Shearer, J.; Zhang, C. X.; Hatcher, L. Q.; Karlin, K. D. *J. Am. Chem. Soc.* **2003**, *125*, 12670–12671.
- (55) Jung, H. H.; Floreancig, P. E. *Tetrahedron* **2009**, *65*, 10830–10836.
- (56) Kolev, J. N.; Zaengle, J. M.; Ravikumar, R.; Fasan, R. *ChemBioChem* **2014**, *15*, 1001–1010.